HHS Public Access

Author manuscript

Phys Med Biol. Author manuscript; available in PMC 2019 August 08.

Published in final edited form as:

Phys Med Biol. 2014 September 21; 59(18): 5225–5242. doi:10.1088/0031-9155/59/18/5225.

THE UF/NCI FAMILY OF HYBRID COMPUTATIONAL PHANTOMS REPRESENTING THE CURRENT U.S. POPULATION OF MALE AND FEMALE CHILDREN, ADOLESCENTS, AND ADULTS – APPLICATION TO CT DOSIMETRY

Amy M. Geyer, MS,
J. Crayton Pruitt Family Department of Biomedical Engineering, University of Florida, Gainesville, FL 32611-6131

Shannon O'Reilly, MS,
J. Crayton Pruitt Family Department of Biomedical Engineering, University of Florida, Gainesville, FL 32611-6131

Choonsik Lee, PhD,
National Cancer Institute, National Institute of Health, Bethesda, MD 20892-1502

Daniel J. Long, PhD,
J Crayton Pruitt Family Department of Biomedical Engineering, University of Florida, Gainesville, FL 32611-6131

Wesley E. Bolch, PhD
J Crayton Pruitt Family Department of Biomedical Engineering, University of Florida, Gainesville, FL 32611-6131

Abstract

Purpose—Substantial increases in pediatric and adult obesity in the United States have prompted a major revision to the current UF/NCI (University of Florida / National Cancer Institute) family of hybrid computational phantoms to more accurately reflect current trends in larger body morphometry.

Methods—A decision was made to construct the new library in a gridded fashion by height/weight without further reference to age-dependent weight/height percentiles as these become quickly outdated. At each height/weight combination, circumferential parameters were defined and used for phantom construction. All morphometric data for the new library were taken from the CDC NHANES survey data over the time period 1999 to 2006, the most recent reported survey period. A subset of the phantom library was then used in a CT organ dose sensitivity study to examine the degree to which body morphometry influences the magnitude of organ doses for patients that are underweight to morbidly obese in body size.

Results—Using primary and secondary morphometric parameters, grids containing 100 adult male height/weight bins, 93 adult female height/weight bins, 85 pediatric male height/weight bins,

For reprints and correspondence contact: Wesley E. Bolch, PhD, PE, CHP, Department of Biomedical Engineering, University of Florida, Gainesville, Florida 32611-8300, Phone: (352) 846-1361 Fax: (352) 392-3380, wbolch@ufl.edu.

and 73 pediatric female height/weight bins were constructed. These grids served as the blueprints for construction of a comprehensive library of patient-dependent phantoms containing 351 computational phantoms.

Conclusions—At a given phantom standing height, normalized CT organ doses were shown to linearly decrease with increasing phantom BMI for pediatric males, while curvilinear decreases in organ dose were shown with increasing phantom BMI for adult females. These results suggest that one very useful application of the phantom library would be the construction of a pre-computed dose library for CT imaging as needed for patient dose-tracking.

Keywords

computational phantom; patient-dependent phantom; obesity; computed tomography

1. Introduction

Computational phantoms are an essential component for documenting patient dose in both medical imaging and radiotherapy. For most nuclear medicine and interventional fluoroscopy procedures, no 3D image of the body is present for dosimetric analysis, and thus organ doses must be derived using these virtual anatomic models. In computed tomography and radiotherapy treatment planning, 3D images are present, but organ contouring can be problematic. Furthermore, phantoms are needed for documenting doses to organs that lie either partially or fully outside the imaging or treatment field. Computational phantoms presently come in one of three format types, and in one of four morphometric categories. Format types include stylized (mathematical equation-based), voxel (segmented CT/MR images), and hybrid (NURBS and polygon mesh surfaces). Morphometric categories include reference (small library of phantoms by age at 50^{th} height/weight percentile), patient-dependent (larger library of phantoms at various combinations of height/weight percentiles), patient-sculpted (phantoms altered to match the patient's unique outer body contour), and finally, patient-specific (an exact representation of the patient with respect to both body contour and internal anatomy).

Figure 1 demonstrates one potential progression in anatomic specificity in medical dosimetry in which one relies first upon reference phantoms (stylized, voxel, and then hybrid formats), moving next to a phantom from a much larger patient-dependent phantom library. Finally, one may wish to utilize phantom sculpting or ultimately create and employ a patient-specific phantom. In the application of computational phantoms for medical dosimetry, however, the need for accuracy must be balanced with practicality. Patient-dependent phantoms provide an acceptable level of accuracy through the modification of reference phantoms to match patient body size and shape, but they remain broad enough to represent a diverse population. Furthermore, as shown in Figure 1, one may construct a pre-computed dose library using patient-dependent phantoms, the most obvious being those for CT and nuclear medicine dosimetry, where the irradiation geometry is nominally fixed and known in advance. For patient-sculpted and patient-specific phantoms, one must commit to a Monte Carlo simulation unique to the patient phantom just created.

As patient-dependent phantoms are typically created through modification of existing phantoms (such as a hybrid reference phantom or a patient-specific voxel phantom), it is advantageous to work with the hybrid phantom format due to its ability to be extensively deformed via NURBS and polygon mesh surface modeling. Utilizing hybrid patient-dependent phantoms, phantom libraries may be created through matching statistically-analyzed anthropometric parameters representing a population of individuals of varying body size and shape. Phantom libraries are useful in radiation protection studies, as well as for pre-computed organ dose libraries, and can be used to analyze changes in tissue dose with varying body morphometry. A brief summary of published phantom libraries is provided here.

Broggio *et al* (2011) constructed a phantom library consisting of 25 whole body adult NURBS-based Caucasian phantoms with 109 identified organs or tissues. Using a sampling strategy, 25 individuals were selected from the European Edition of the Civilian American and European Surface Anthropometry Resource (CAESAR) database.[1] The CAESAR database provides a mesh geometry of the outer body contour for individual volunteers subjected to exterior optical scanning. These body contours were then subsequently converted to NURBS surfaces for inclusion in the CAESAR library. Internal organs for the models were taken from the commercially-available organ sets provided by 3DSpecial [2] and were resized using scaling factors incorporated into each model. The body contour, internal organs, and skeletal models were subsequently voxelized and merged to create the final whole body adult phantom library.

In a study by Na *et al* (2010), percentile-specific phantoms were created using computer algorithms to deform previously constructed reference phantoms (RPI-adult male and RPI-adult female). The internal organs within the phantoms were created using a commercial organ mesh dataset, Anatomium™ 3D,[3] and were scaled using computer algorithms to match volume and mass percentiles derived from International Commission on Radiological Protection (ICRP) Publications 23 and 89 (ICRP, 1975, 2002). To create varying whole-body sizes, anthropometric data (height and weight percentiles) for 19-year-old males and females were derived from the National Health and Nutrition Examination Survey (NHANES) database (1999–2002) and these parameters were matched by deforming another commercially available skin model, MakeHuman™.[4]

In 2012, Ding *et al* extended the RPI-adult male and female computational phantom libraries to include obese patients. The library contains 10 phantoms (5 male and 5 female) created through modifications to the RPI-adult male and RPI-adult female phantoms (Ding *et al.*, 2012). The outer body surface of the RPI-adult male and female was deformed according to anthropometric data from Smith *et al* (2001) and Camhi *et al* (2011) to simulate an increase in subcutaneous fat. An increase in visceral fat was modeled using the relationship between waist circumference and visceral fat outlined in Camhi *et al.* (2011). For each gender,

[1] http://store.sae.org/caesar/index.htm
[2] http://www.3dspecial.com/
[3] http://www.anatomium.com
[4] http://www.makehuman.org/

phantoms were created representing five weight classifications, including normal-weight, over-weight, obese level-I, obese level-II, and morbidly obese.

Cassola *et al* (2011) created a library of 18 anthropometric phantoms (9 adult male phantoms and 9 adult female phantoms) based on 10th, 50th, and 90th mass and height percentiles of Caucasian individuals, extracted from the commercially available ergonomic software PeopleSize.[5] The 3D modeling software Blender was used to deform previously constructed base phantoms, MASH3_sta (male adult mesh – standing) and FASH3_sta (female adult mesh – standing), to match the extracted height and weight parameters (Cassola *et al.*, 2010). To resize internal anatomy, scaling factors were derived as a function of height based on an autopsy study reported in de la Grandmaison *et al.* (2001).

Segars *et al* (2013) extended their original XCAT models, creating a library of 58 adult 4D XCAT phantoms varying in BMI. The 35 adult male and 23 adult female phantoms were created through segmentation of several organs and structures, combined with previously constructed XCAT phantoms. PeopleSize software was used, based on BMI percentile matching, to determine facial measurements, as well as arm length, upper and lower arm skin circumferences, and upper and lower leg skin circumferences.

In 2009, Johnson et al developed the first library of patient-dependent phantoms based upon the UF/NCI (University of Florida / National Cancer Institute) series of ICRP Publication 89 compliant hybrid phantoms of the male and female newborn, 1-year-old, 5-year-old, 10-year-old, 15-year-old, and adult (Lee *et al.*, 2010). The methodology was based on pediatric and adult anthropometric percentile distributions from the NHANES III database of the U.S. Centers for Disease Control and Prevention (CDC) covering the survey period 1988 to 1994.[6] Patient-dependent phantoms were then created by modifying various UF/NCI hybrid reference phantoms to match predefined anthropometric parameters. In total, Johnson *et al* created 25 adult male, 25 adult female, 50 pediatric male, and 50 pediatric female patient-dependent phantoms.

In 2010, the Centers for Disease Control and Prevention (CDC) estimated that roughly 12.5 million (17%) children and adolescents (ages 2–19) are obese in the United States, almost tripling the childhood obesity rate since 1980.[7] Furthermore, CDC reports that as of 2010, adult obesity rates exceed 30% of the adult population in no fewer than 12 of the 50 U.S. states.[8] These rates are substantially higher than what was reflected in the body morphometry statistics of the NHANES III database some 15 years prior. With these large increases, it was thus necessary to update the data from Johnson *et al* (2009) to reflect these changes. At the same time, it was necessary to abandon the previous method of age-based percentile calculations as height/weight percentiles become increasingly outdated with these increasing obesity trends.

[5] http://www.openerg.com/psz
[6] http://www.cdc.gov/nchs/nhanes.htm
[7] http://www.cdc.gov/obesity/childhood/data.html
[8] http://www.cdc.gov/obesity/data/adult.html

The purpose of the present study was thus to create four comprehensive libraries of patient-dependent phantoms that more appropriately reflect current U.S. body morphometry data: pediatric males, pediatric females, adult males, and adult females. Ranges for heights and weights within each of the four grids were selected to encompass their 5^{th} and 95^{th} percentile values. For each phantom library, height/weight grids were constructed for which statistical averages of CDC-sampled body circumferences and sitting heights were assigned at each height/weight combination. To demonstrate the utility of the new phantom libraries, a subset of pediatric male and adult female phantoms were used to investigate the correlation of CT organ dose on changes in phantom weight at selected standing heights.

2. Materials and Methods

2.1 Statistical Analysis of NHANES Data

Anthropometric adult and pediatric data were obtained from the NHANES database conducted between 1999 and 2006 (referred to as the NHANES IV database). At the time of this study, 2006 was the most recent data available for analysis. Height and weight were chosen as primary parameters in the construction of grids for adult males and adult females covering ages of 20 to 85 years (total of 17,483 individuals). Similarly, the same primary parameters were used in the construction of grids for pediatric males and females aged 2 to 20 years (total of 17,028 individuals). Waist, thigh, and arm circumferences were included as secondary parameters. Due to the unavailability of sitting height and buttocks circumference in the database applied in this study, average values of these additional parameters were interpolated from the prior NHANES III database as matched the heights and weights of individuals in the updated grids.

Male and female pediatric individuals were analyzed independently and binned in height increments of 10 cm, ensuring that the 5th and 95th height percentiles were captured as per a MATLAB Gaussian fitting program. Each height bin was further parsed by weight increments of 5 kg, with each weight bin containing data for at least ten individuals to assure statistical significance. For each height-weight bin, secondary parameters including the average circumferences of the arm, waist, and thigh were determined, along with sitting height and buttocks circumference from the previous NHANES database. For a small number of weight extremes, not all secondary parameters contained the necessary ten individuals, and thus linear extrapolation was used to determine appropriate values. Using primary and secondary parameters, a grid containing 85 male height/weight bins and a grid containing 73 female height/weight bins were thus constructed as shown in Figure 2.

A similar statistical analysis of data was performed to create the adult grids with the exception that the height binning was performed at 5 cm, due to the smaller range of heights in the sampled population. As a result, a grid containing 100 male height/weight bins and a grid containing 93 female height/weight bins were constructed as shown in Figure 3. These grids served as the blueprints the construction of a composite library of patient-dependent phantoms containing a total of 351 adult and pediatric phantoms.

2.2 Reshaping of UF/NCI Reference Phantoms

As outlined below in Section 2.4, the UF/NCI family of reference hybrid phantoms are utilized in this study as the initial anatomic models for creation of the larger phantom library. In the study by Lee et al which documents their creation, a variety of data sources were used for targeted body circumferences, many of which are found to no longer be compatible with values given in our statistical analysis of the NHANES IV survey data. Consequently, an effort was made to first reshape the body contour of those reference phantoms used in this study (see Table 1).

To begin this update, the primary parameters of height and weight were left unchanged from their ICRP Publication 89 reference values, while the circumference parameters were revised. This process included a double linear interpolation of the circumference data. The first interpolation was performed to match the ICRP reference weight, while the second interpolation was to match reference height. In cases that lacked sufficient circumferential data to allow for interpolation, extrapolation based on the least squares method was used to obtain the targeted body circumference. Updated circumferences were calculated for each phantom in the current UF/NCI reference phantom library, excluding the newborn and 1 year old since data at these ages were not available from either the NHANES III or IV databases.

After calculating updated circumference data, the UF/NCI reference phantoms were modified accordingly. Body region circumferences for each phantoms were matched to within 3% of targeted values. Other body region adjustments were made to then re-match ICRP reference organ masses to within 1%.

2.3 Body Mass Index Analysis

To further aid in the construction of the extended UF/NCI phantom library, body mass index (BMI) calculations were performed at each height/weight bin within the four phantom grids. As the scaling of phantoms can be quite labor-intensive, requiring additional steps for overweight individuals (detailed in a later section), it was useful to know the weight category (underweight, healthy, overweight, or obese) prior to the scaling process. An individual's BMI is a reliable indication of weight category and is formally defined as the ratio of the body mass to the square of the body height (in units of kg m-2). For adults, this calculated number would then fall within a CDC-defined an acceptable range for each weight category. Underweight individuals have a BMI below 18.5, while healthy individuals have a BMI within the range 18.5 – 24.9. Overweight, obese, and morbidly obese individuals have BMI values between 25.0 – 29.9, between 29.9 – 39.9, and exceeding 40.0, respectively. Once BMI values and categories were assigned to each height-weight combination, the adult grids of Figure 3 were then color-coded based on these weight categories.

For pediatric individuals, weight categories are not determined directly by BMI due to body developmental changes during growth years, but are instead defined based on BMI percentiles. To determine a weight category for pediatric subjects, an average age of the individual in each height/weight bin was estimated for both the males and female grids. For each BMI value and average age, BMI-for-age charts provided by CDC were used to

determine a BMI percentile for each individual. BMI values below the 5th percentile are considered underweight individuals, while BMI values ranging between the 5th percentile and 85th percentiles represent healthy individuals. BMI values ranging between the 85th and 95th percentiles are considered overweight, while BMI values falling above the 95th percentile are considered obese. The pediatric grids of Figure 2 were also color-coded based on these various weight categories.

2.4 Phantom Scaling Process

The scaling process in this study mimics that previously established by Johnson *et al* (2009), and begins through modification of an appropriate member of the 12-phantom UF/NCI reference library of Lee *et al* (2010). The process is demonstrated in Table 1 where 11 values of pediatric phantom standing height and 9 values of adult phantom standing height are targeted within the expanded phantom library. Shown in Table 1 are the acronyms of the individual UF/NCI reference phantoms that are either up-scaled (⬆) or down-scaled (⬇), respectively, to establish an intermediate (or "anchor") phantom at the appropriate standing and sitting height (rows in Figures 2 and 3). These height-adjusted "anchor" phantoms are then further modified across targeted phantom weights (columns in Figures 2 and 3) through increases or decreases in their outer body contour (i.e., subcutaneous fat layer) with additional constraints on CDC-sampled body circumferences. In the end, an array of phantoms are created that are now indirectly coupled to subject age, but more importantly represent the average body morphometry of a person in that height/weight/gender combination as seen in the current U.S population. Further details of this process are given below.

Initially, the sitting height of the appropriate UF/NCI reference phantom is measured as the distance from the top of the head to the bottom of the ischium. A scaling factor is then defined as the ratio of the targeted to measured sitting height. The head, arms, and torso (including all internal soft tissue and bony anatomy – discussed further below) are then scaled uniformly in 3D by this factor, with the bottom of the ischium acting as the point of origin. To match a targeted standing height, the legs are next scaled in the z-direction, again by the ratio of measured to targeted values. With proper standing and sitting heights matched within the anchor phantom, circumferential parameters are then matched to create phantoms across each row of the grid as shown in Figs 2 and 3.

To ensure consistency, reference control points are established at locations matching CDC's measurements of these same parameters in their NHANES surveys. Control points on the outer body contour are modified to simulate changes in subcutaneous adipose thickness to match targeted body circumferences. For phantoms with waist circumferences smaller than that of a given anchor phantom, a 2D scale is applied in the x-y plane to accommodate this change while preserving the targeted standing height. For heavier phantoms, the arms are rotated outward slightly to avoid overlap with the outer body contour. Once body circumferences are matched, control points adjacent to those defining the body circumference measurements are visually analyzed and fine-tuned to preserve appropriate body shapes. To complete the phantom scaling process, total body mass is iteratively matched through adjusting control points on the outer body contour in areas not restricted by

secondary parameters. These include the lower arms and legs, upper torso and neck, and adipose tissue layer of the breasts (in females). Total body mass is estimated in the NURBS modeling software Rhinoceros™ using a volume calculation tool and ICRU Report 46 tissue densities (ICRU, 1992).

As shown in Table 1, all phantoms within the revised UF/NCI phantom library trace their origin to the hybrid versions of the ICRP reference phantoms, which in turn incorporate age and/or gender dependent reference organ masses, matched to within 1% of ICRP Publication 89 values as described by Lee *et al* (2010). Once the torso of a given reference phantom is increased or decreased through 3D (or possibly 2D) scaling, these reference organ masses are proportionally increased or decreased as well. This approach was discussed at length by Johnson *et al* (2009) and was empirically confirmed by the cadaver studies of de la Grandmaison *et al*. (2001) in which larger individuals tended to display larger organs, although individual variations at a given cadaver BMI were quite large. It is thus impractical if not impossible to establish "reference" organ masses at different body sizes (height/weight combinations) beyond those established for the limited ICRP reference phantoms. The more important feature of the expanded UF/NCI phantom library, as well as in other published phantom libraries, is that they no longer restrain the user to a limited set of reference phantoms, but allow explicit treatment of body morphometry variations as seen in actual patient populations. Further improvements in organ dosimetry would necessitate explicit knowledge of organ mass, shape, and depth within the body for each patient, which in many cases, will be impossible to obtain short of establishing a patient-specific phantom (see Figure 1).

2.5 Simulated Computer Tomography Exams

The effect of body morphometry on organ doses for a chest-abdomen-pelvis (or CAP) CT scan was assessed by simulating a Toshiba Aquilion One CT scanner using the Monte Carlo transport code MCNPX2.6 and performed on 22 phantoms. The influence of body size on organ doses was assessed using 16 adult female phantoms from the expanded UF/NCI library at weight increments of 5 kg, starting with 50 kg, at a fixed height of 170 cm. Additionally, six pediatric male phantoms at weight increments of 5 kg, starting at 25 kg, at a fixed standing height of 135 cm were selected. All phantoms were voxelized to a resolution of $2 \times 2 \times 2$ mm3. The scan parameters for the adult female phantoms were beam energies of 120 and 135 kVp, large beam-shaping (bowtie) filter, pitch of 0.828, 100 mAs/rotation, and a 3.2 cm beam collimation. The scan parameters for the pediatric male phantoms were beam energies of 100 and 120 kVp, medium beam-shaping filter, pitch of 0.828, 100 mAs/rotation, and a 3.2 cm beam collimation. All scans ranged from the thoracic inlet to the lesser trochanter on each phantom, with arms removed from each phantom to mimic clinical conditions in which the patients would be positioned with their arms raised above their head for the examination. The MCNP source term model for the Toshiba Aquilion One was established using the equivalent spectrum method of Turner et al (2009) and validated within relative errors of ±5% using both head and body CTDI phantoms (Long, 2013).

3. Results

3.1 Obesity Trends

Statistical reviews of body morphometry data from both the NHANES III (1988 – 1994) and the more recent NHANES IV (1999 – 2006) surveys are shown in Tables 2 and 3 for pediatric and adult subjects, respectively. These tables give the percentage of individuals at various standing heights that are either obese or (for adults) morbidly obese. As shown in Table 2, increases in these percentages across the two survey periods are demonstrated at all pediatric standing heights with the exception of 85 cm for males, and 85 and 125 cm for females. The average percent increase in the proportion of obese children across all height categories are shown to 34% and 23% for males and females, respectively, for the NHANES III versus NHANES IV survey periods. In Table 3, increases in the proportion of obese adults between the two sampling periods are shown to be consistently high at all targeted standing heights, with average percent increases of 41% for adult males and 24% for adult females across the two sampling periods. These results give clear indication for the expanded and revised UF/NCI phantom library, as well as the movement away from a percentile naming system for the phantom library to one based upon height/weight grids driving phantom construction.

3.2 Updated Reference Phantoms

Data collected from the NHANES IV database were used to update the UF/NCI reference phantoms of Lee et al (2010) with respect to body circumference data. Targeted values were interpolated from the database at each ICRP 89 reference standing height and total body mass. These updates also corrected for anatomical discrepancies in the phantom outer body shape. Previously, the buttocks circumference in the phantoms, with the exception of the 15-year and adult female phantoms, was found to be less than the corresponding waist circumference, a trend not consistent with the NHANES IV database. Table 4 shows current, targeted, and revised circumferential data for all reference phantoms used in this study. For consistency, all circumference measurements were made using previously discussed CDC-defined measurement planes. The revised circumferences were matched to suggested updated dated values to within 3%. Once circumferences were matched, organ masses, total body mass and separable fat mass were matched to within 1% of ICRP 89 reference values.

3.3 Phantom Library Grids and Phantom Library

The final height/weight grids for pediatric and adult males/females are show in Figures 2 and 3, respectively. For the pediatric phantoms, the grids are color-coded to indicate the phantom classification as either underweight, healthy, overweight, or obese based on BMI percentile analyses using CDC definitions of body morphometry. For the adult grids, an additional category of morbidly obese was added. In total, the grids display height/weight combinations for 100 adult male, 93 adult female, 85 pediatric male, and 73 pediatric female phantoms. Each height/weight grid element corresponds to a unique phantom in the expanded library matched to targeted values of sitting height and four body circumferences – waist, buttocks, arm, and thigh. For each phantom, total body mass was matched to within 1 kg, total height matched to within 1 cm, and all circumferential values matched to within 1% of targeted values. In Figures 2 and 3, some combinations of height and weight are not

color-coded indicating body morphometries that were poorly sampled in the NHANES IV database. For these combinations, no statistically reliable body circumferential data were available for phantom construction. Future extensions of the UF/NCI phantom libraries will thus have to rely on extrapolated data, and/or additional sampling.

3.4 Patient-Dependent Phantom Library Subset for CT Dosimetry

A subset of patient-dependent phantoms was selected from the male pediatric grid and female adult grid to explore the impact of body mass on organ doses in CT examinations. For this purpose, 16 adult female patient-dependent phantoms were selected at a fixed standing height of 170 cm, with body masses ranging from 50 kg to 125 kg in 5-kg increments. Additionally, 6 pediatric male patient-dependent phantoms were selected at a fixed standing height of 135 cm with body masses ranging from 25 kg to 50 kg in 5 kg increments. These adult female and pediatric male phantoms are displayed in Figures 4 and 5, respectively. All phantoms were voxelized using the MATLAB™ code Voxelizer v9.2 (Lee *et al.*, 2010). Monte Carlo CT simulations were then performed for all 22 patient-dependent phantoms to investigate the influence of body mass on CT organ dose. Normalized organ dose, in units of mGy per 100 mAs per rotation, are shown as a function of phantom BMI in Figure 6 for lungs, heart, liver, and spleen, and in Figure 7 for kidneys, thyroid, breast, an active marrow.

4. Discussion

4.1 Phantom Organ Masses and Naming Convention

A summary of masses for five primary organs within the field of view of the CAP computed tomography scan are given in Table 5. Both NURBS-based (pre-voxelization) and voxelized (post-voxelization) masses are given, with differences shown to be within ±2.2% for all organs. As discussed previously in Section 2.4, organ masses remain constant at a given standing height as per the 3D scaling the source reference phantom (see Table 1). For those underweight and healthy patient phantoms where additional 2D scaling was employed to match targeted body circumferences, organ masses are shown to decrease. The naming convention for phantoms from the expanded UF/NCI library begins with the identifier UFH (University of Florida Hybrid), followed by two capital letters – PM, PF, AM, or AF (pediatric male, pediatric female, adult male, or adult female), and then the phantom standing height and total body mass in cm and kg, respectively.

4.2 BMI Variations in CT Organ Doses

The data of Figures 6 and 7 confirm that organ doses – under fixed tube currents and normalized to 100 mAs per rotation – decrease with increasing phantom BMI in a fairly consistent pattern (with the exception of the thyroid). Normalized organ doses for the 135-cm pediatric males generally demonstrate linear decreases with increasing phantom BMI, while normalized organ doses for the 170-cm adult females decrease along a more curvilinear/quadratic relationship with increasing phantom BMI. In both cases, normalized organ doses are higher at higher and more penetrating tube potentials.

The slight "rippling" of the data can be attributed to the unique body morphometry of each member of the phantom series as defined by both the NHANES IV statistical averages for body circumferences at each height/weight combination, as well as finer specifics of the phantom scaling process. Of all the organs considered in this study, only the thyroid shows significant discontinuities with changes in phantom BMI. This organ is located at juncture of the neck and upper torso, and is very near the start of the CT scan range. The radiation dose received by the thyroid is thus greatly influenced by scatter and attenuation of the CT x-ray field with variations in upper chest and neck thickness across the BMI values considered in this phantom subset.

The trends in organ dose as a function of increasing BMI shown in Figures 6 and 7 are limited to those for a fixed value of phantom standing / sitting height. As noted in Section 2.4, the organ masses in the UF/NCI phantom library along a given row of phantom height (Figures 2 and 3) are equivalent, and only the subcutaneous fat layer of the phantom changes for each column of phantom weight. Consequently, any predictive equation of CT organ dose with BMI as inferred from Figures 6 and 7 would have to repeated for each value of phantom height. Variations of organ dose with increasing BMI at a fixed weight but variable height do not show in any predictive pattern as body size and organ mass vary accordingly.

4.3 Limitations of the Current Library

There are two major limitations to the newly expanded UF/NCI phantom library. First, changes in phantom mass at each targeted standing height were made based solely on changes in the thickness of subcutaneous fat. While this is a reasonably approximation for pediatric individuals, increases in phantom BMI for adult phantoms should additionally consider changes in visceral fat. Second, breast size was increased in the phantoms of this study as monotonically increasing functions of phantom weight for both adult and pediatric female phantoms at standing heights 155 cm and above. Figure 8 demonstrates this trend for the 155-cm adult female phantoms. As breast size was not sampled within the NHANES IV database, other data sources should be sought to establish more definitive statistical averages of breast size correlated to subject height and weight.

5. Conclusions

Following increasing obesity trends in the United States among both adults and pediatric individuals, a significant expansion of the earlier UF/NCI family of patientdependent hybrid phantoms was warranted and thus undertaken in this study using CDC sampling data for the period 1999 to 2006. The resulting expanded phantom library was constructed along four height/weight grids – 85 pediatric males, 73 pediatric females, 100 adult males, and 93 adult females – with each phantom corresponding to a unique combination of standing and body weight and covering their 5^{th} and 95^{th} percentiles values. Secondary morphometric parameters used in phantom construction included sitting height and body circumference for waist, buttock, arm, and thigh. A subset of the phantom series was then used to explore variations in normalized CT organ dose with increases in phantom BMI. At a given phantom standing height, normalized CT organ doses were shown to linearly decrease with increasing phantom BMI for pediatric males, while a curvilinear decrease was shown with increasing

phantom BMI for adult females. These preliminary results suggest that one very useful application of the phantom library would be the construction of a pre-computed dose library for CT imaging as needed for patient dose-tracking, an effort presently ongoing at the University of Florida.

ACKNOWLEDGMENTS

This work was supported by Contracts HHS-N2612–0090-0098P and HHS-N2612–0100-0692P with the Radiation Epidemiology Branch of the National Cancer Institute, and by a grant from the Biomedical Research and Education Foundation.

This work was supported by

Radiation Epidemiology Branch, Division of Cancer Epidemiology and Genetics, National Cancer Institute

REFERENCES

Broggio D, Beurrier J, Bremaud M, Desbree A, Farah J, Huet C and Franck D 2011 Construction of an extended library of adult male 3D models: rationale and results Phys Med Biol 56 7659–7662 [PubMed: 22086354]

Camhi SM, Bray GA, Bouchard C, Greenway FL, Johnson WD, Newton RL, Ravussin E, Ryan DH, Smith SR and Katzmarzyk PT 2011 The relationship of waist circumference and BMI to visceral, subcutaneous, and total body fat: sex and race differences Obesity (Silver Spring) 19 402–408 [PubMed: 20948514]

Cassola VF, Lima VJ, Kramer R and Khoury HJ 2010 FASH and MASH: female and male adult human phantoms based on polygon mesh surfaces: I. Development of the anatomy Phys Med Biol 55 133–162 [PubMed: 20009183]

Cassola VF, Milian FM, Kramer R, de Oliveira Lira CA and Khoury HJ 2011 Standing adult human phantoms based on 10th, 50th and 90th mass and height percentiles of male and female Caucasian populations Phys Med Biol 56 3749–3772 [PubMed: 21628776]

de la Grandmaison GL, Clairand I and Durigon M 2001 Organ weight in 684 adult autopsies: new tables for a Caucasoid population Forensic Sci Int 119 149–154 [PubMed: 11376980]

Ding A, Mille MM, Liu T, Caracappa PF and Xu XG 2012 Extension of RPI-adult male and female computational phantoms to obese patients and a Monte Carlo study of the effect on CT imaging dose Phys Med Biol 57 2441–2459 [PubMed: 22481470]

ICRP 1975 ICRP Publication 23: Report on the Task Group on Reference Man, (Pergamon Press, Oxford, UK: International Commission on Radiological Protection)

ICRP 2002 ICRP Publication 89: Basic anatomical and physiological data for use in radiological protection - reference values Ann ICRP 32 1–277

ICRU 1992 ICRU Report 46: Photon, electron, proton and neutron interaction data for body tissues, (Bethesda, MD: International Commission on Radiation Units and Measurements)

Johnson P, Whalen S, Wayson M, Juneja B, Lee C and Bolch W 2009 Hybrid patient-dependent phantoms covering statistical distributions of body morphometry in the US adult and pediatric population Proc IEEE 97 2060–2075

Lee C, Lodwick D, Hurtado J, Pafundi D, Williams JL and Bolch WE 2010 The UF family of reference hybrid phantoms for computational radiation dosimetry Phys Med Biol 55 339–363 [PubMed: 20019401]

Long DJ 2013 Monte Carlo calculations of patient organ doses in Toshiba computed tomography examinations with automatic tube current modulation: A feasibility study In: Biomedical Engineering, (Gainesville, Florida: University of Florida) p 152

Na YH, Zhang B, Zhang J, Caracappa PF and Xu XG 2010 Deformable adult human phantoms for radiation protection dosimetry: anthropometric data representing size distributions of adult worker populations and software algorithms Phys Med Biol 55 3789–3811 [PubMed: 20551505]

Segars WP, Bond J, Frush J, Hon S, Eckersley C, Williams CH, Feng J, Tward DJ, Ratnanather JT, Miller MI, Frush D and Samei E 2013 Population of anatomically variable 4D XCAT adult phantoms for imaging research and optimization Med Phys 40 043701 [PubMed: 23556927]

Smith SR, Lovejoy JC, Greenway F, Ryan D, deJonge L, de la Bretonne J, Volafova J and Bray GA 2001 Contributions of total body fat, abdominal subcutaneous adipose tissue compartments, and visceral adipose tissue to the metabolic complications of obesity Metabolism: clinical and experimental 50 425–435 [PubMed: 11288037]

Turner AC, Zhang D, Kim HJ, DeMarco JJ, Cagnon CH, Angel E, Cody DD, Stevens DM, Primak AN, McCollough CH and McNitt-Gray MF 2009 A method to generate equivalent energy spectra and filtration models based on measurement for multidetector CT Monte Carlo dosimetry simulations Med Phys 36 2154–2164 [PubMed: 19610304]

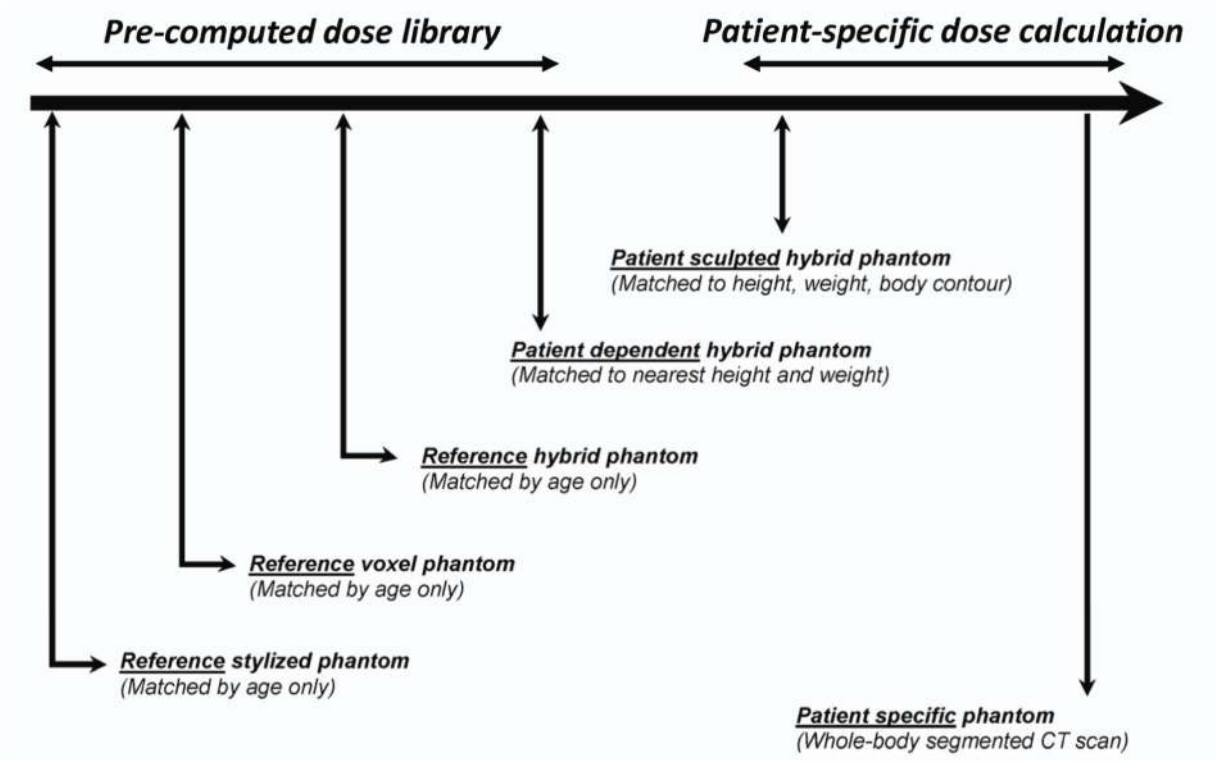

Figure 1.

Diagram of anatomic specificity for medical organ dosimetry in which phantoms of different format types (stylized, voxel, hybrid) and morphometric category (reference, patient-dependent, patient-sculpted, and patient-specific) may be employed.

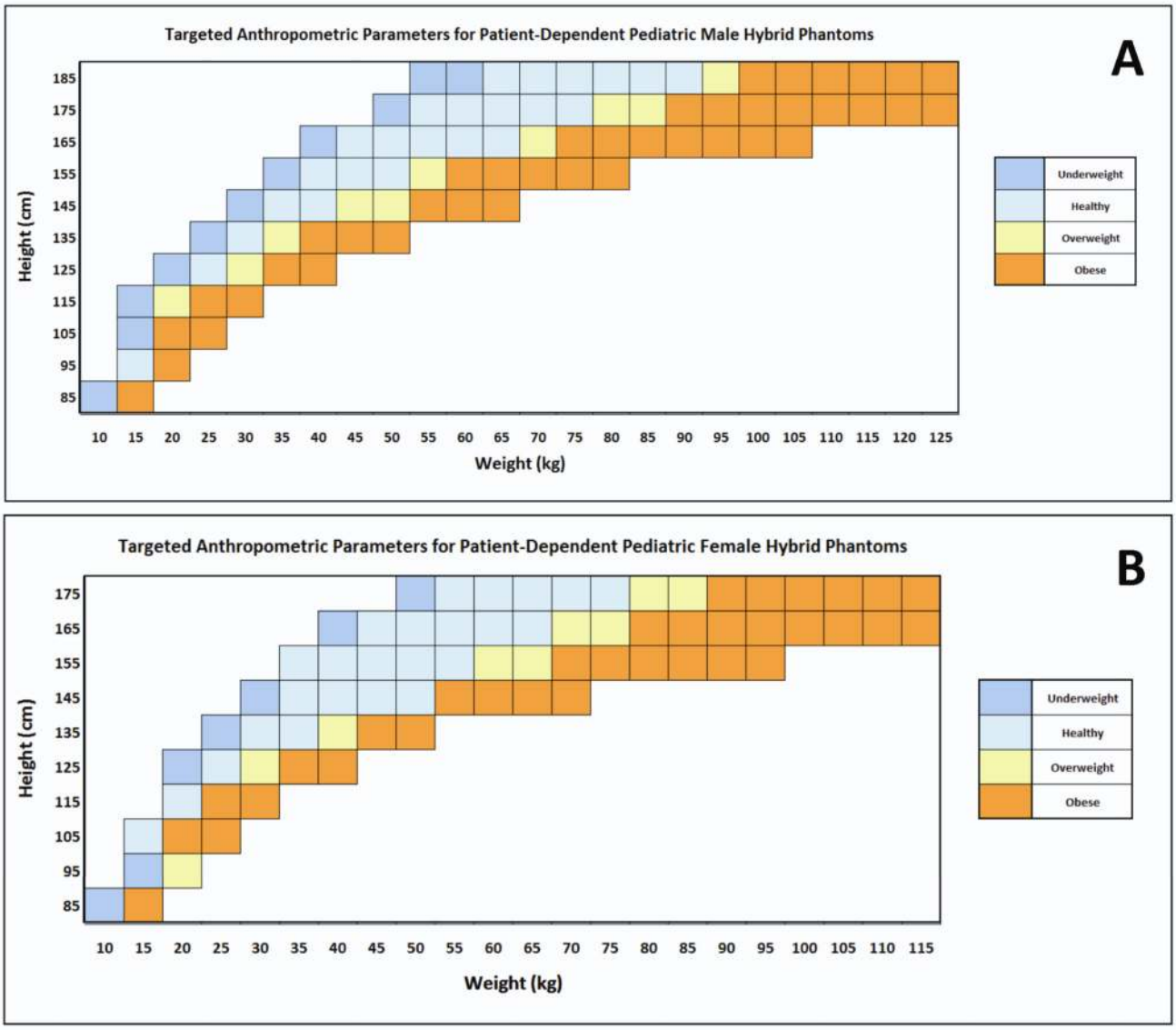

Figure 2.

Targeted grid for the UF/NCI library of **(A)** pediatric male and **(B)** pediatric female hybrid phantoms. Color code indicates the phantom classification as underweight, healthy, overweight, or obese based upon BMI percentiles and CDC definitions of body morphometry.

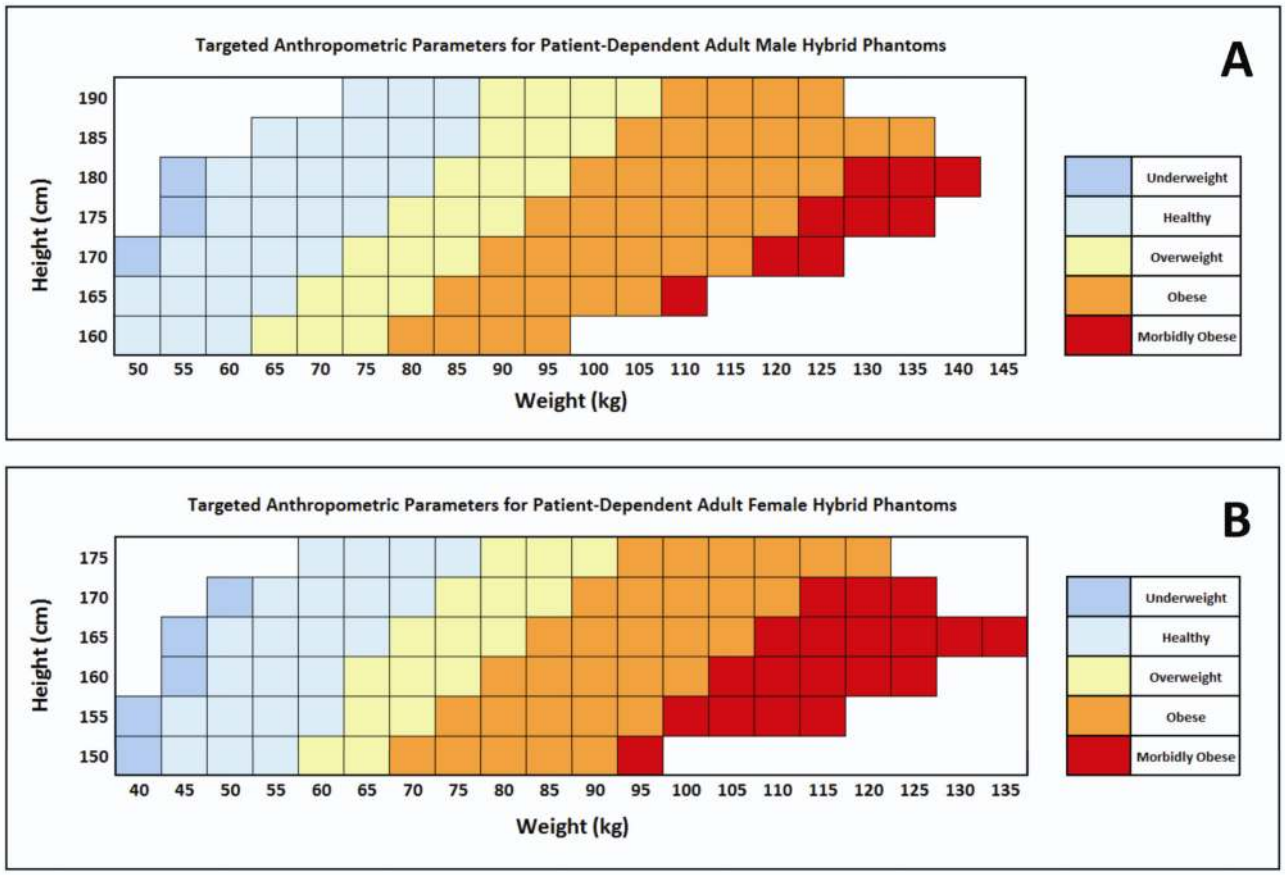

Figure 3.

Targeted grid for the UF/NCI library of **(A)** adult male and **(B)** adult female hybrid phantoms. Color code indicates the phantom classification as underweight, healthy, overweight, obese, or morbidly obese based upon BMI definitions of body morphometry.

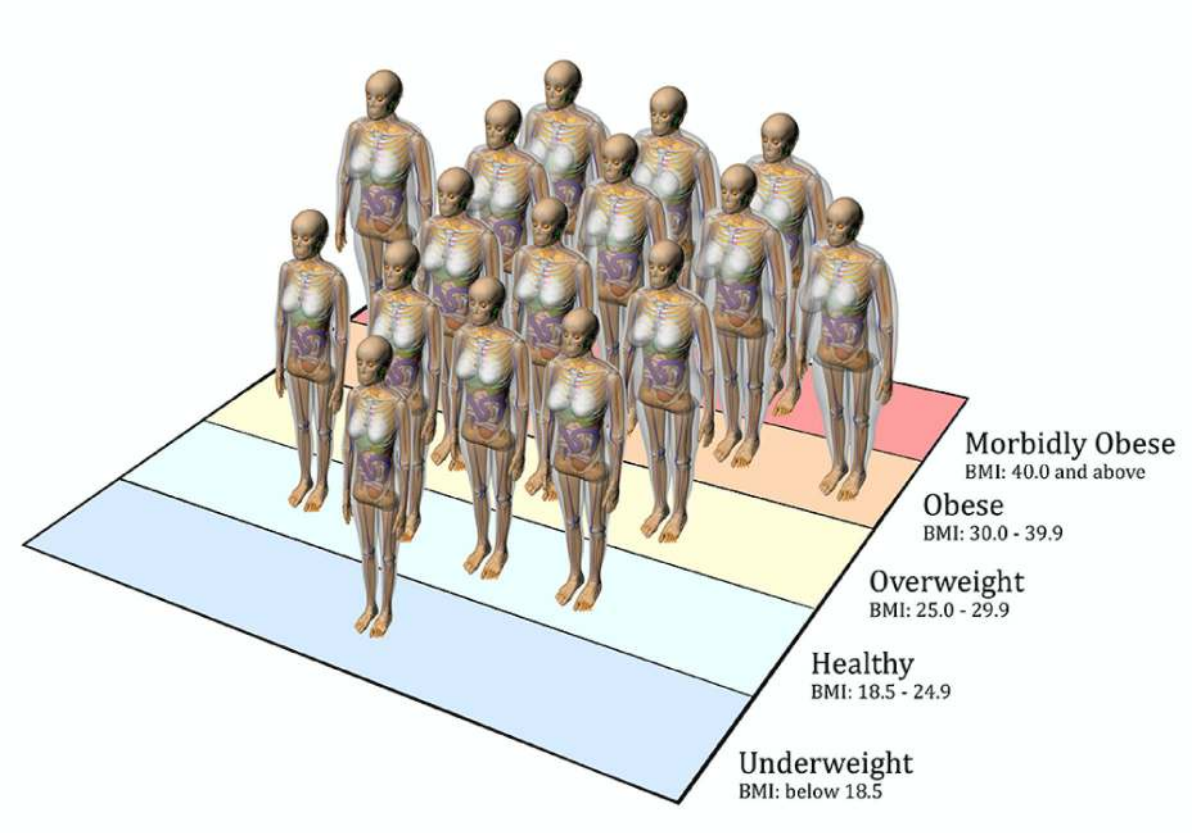

Figure 4.
Selection of adult female phantoms at a fixed height of 170 cm at varying weights.

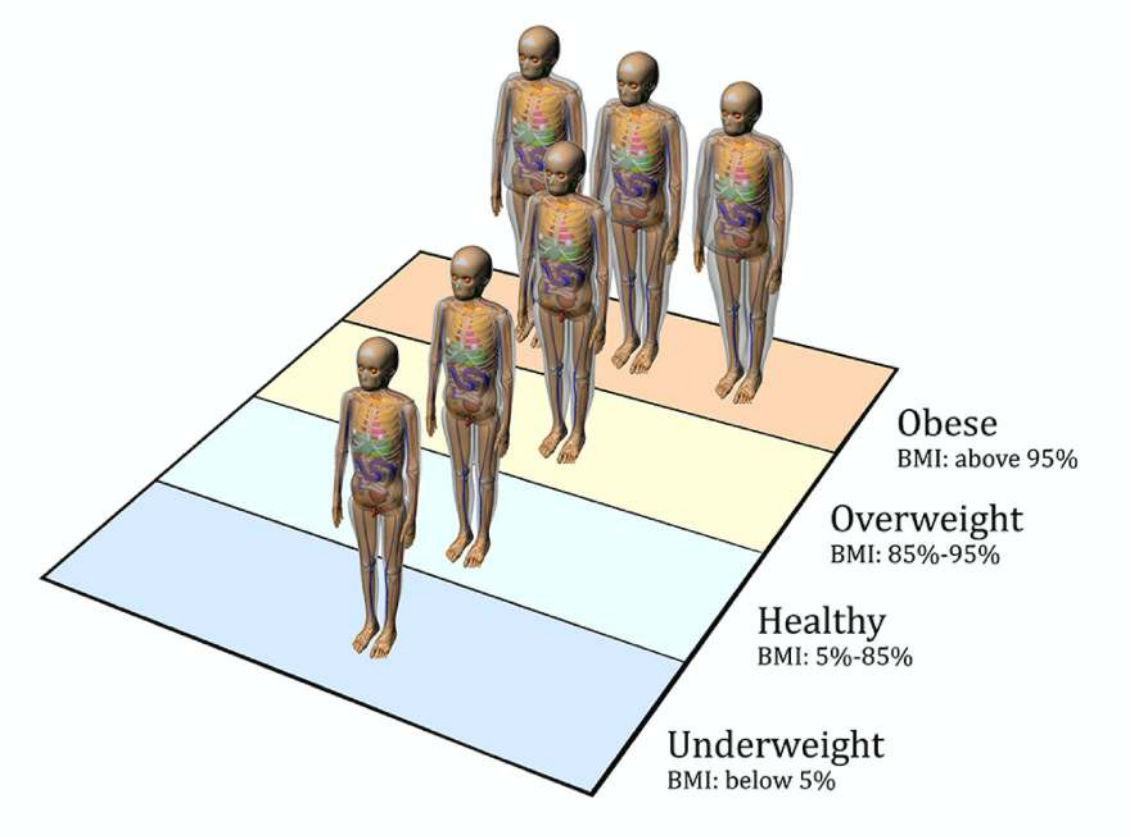

Figure 5.
Selection of pediatric male phantoms at a fixed height of 135 cm at varying weights.

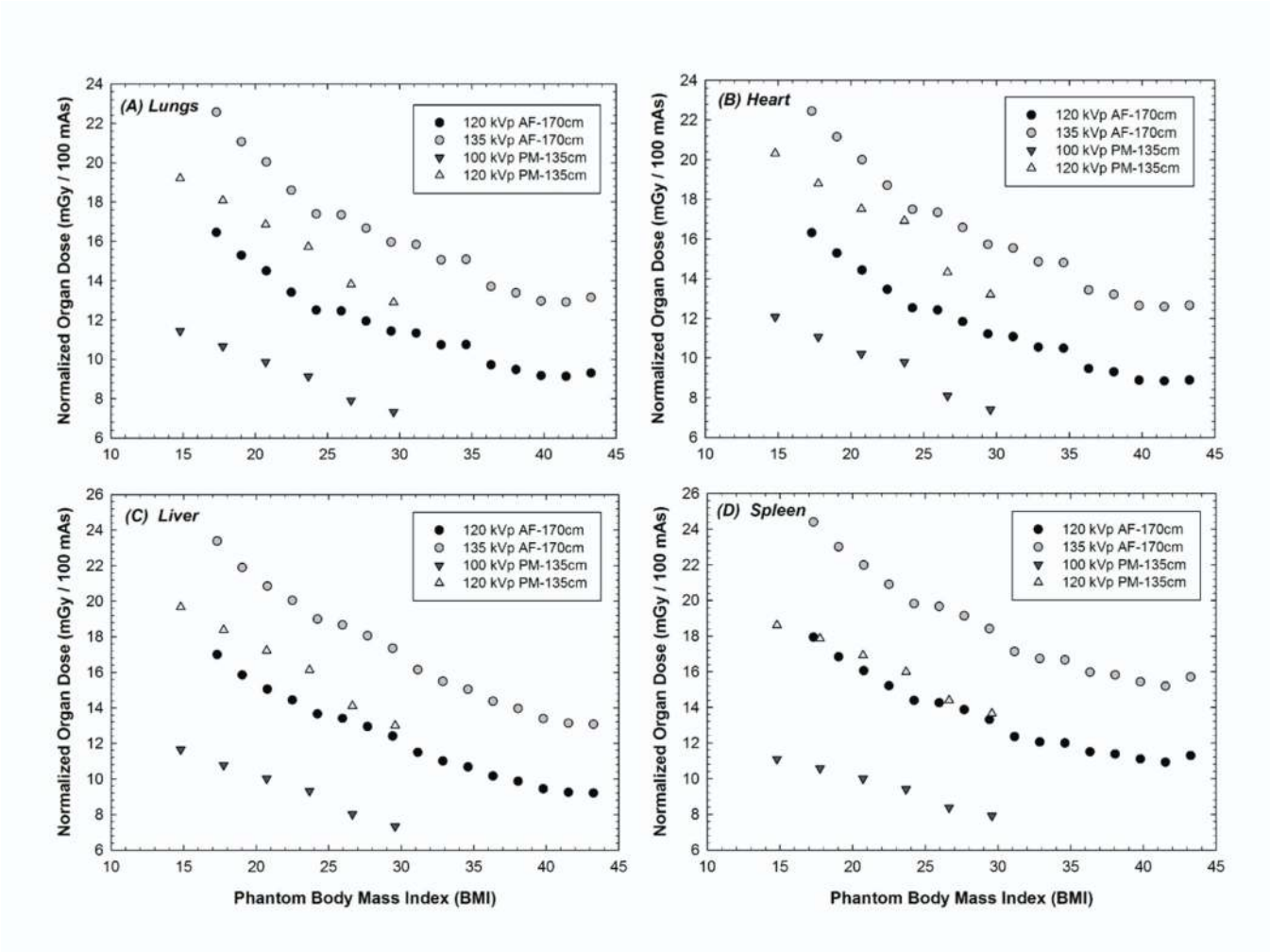

Figure 6.

Variations in absorbed dose to **(A)** lungs, **(B)** heart, **(C)** liver, and **(D)** spleen as a function of BMI for pediatric male and adult female phantoms.

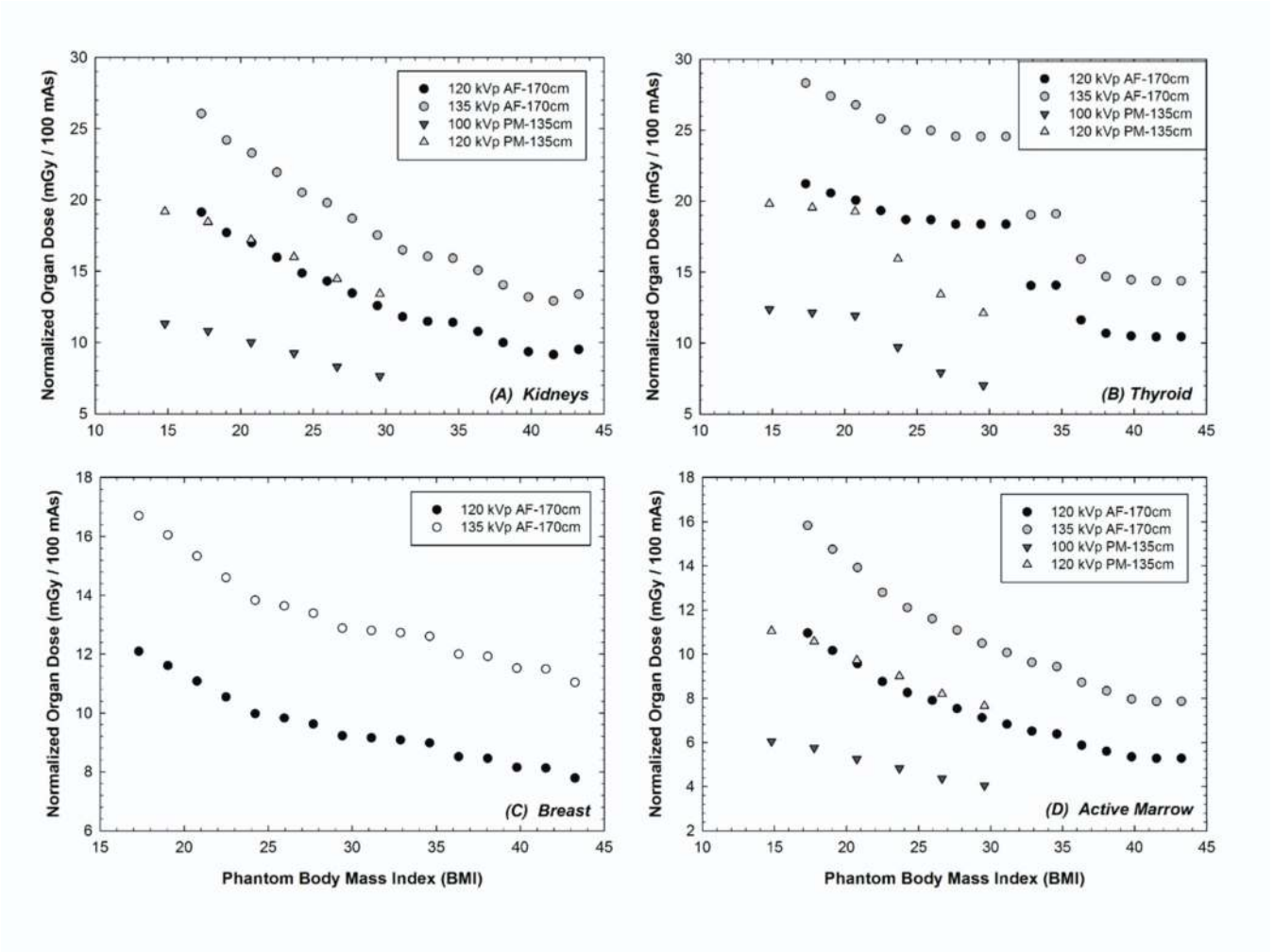

Figure 7.

Variations in absorbed dose to **(A)** kidneys, **(B)** thyroid, **(C)** breast, and **(D)** active marrow as a function of BMI for pediatric male and adult female phantoms.

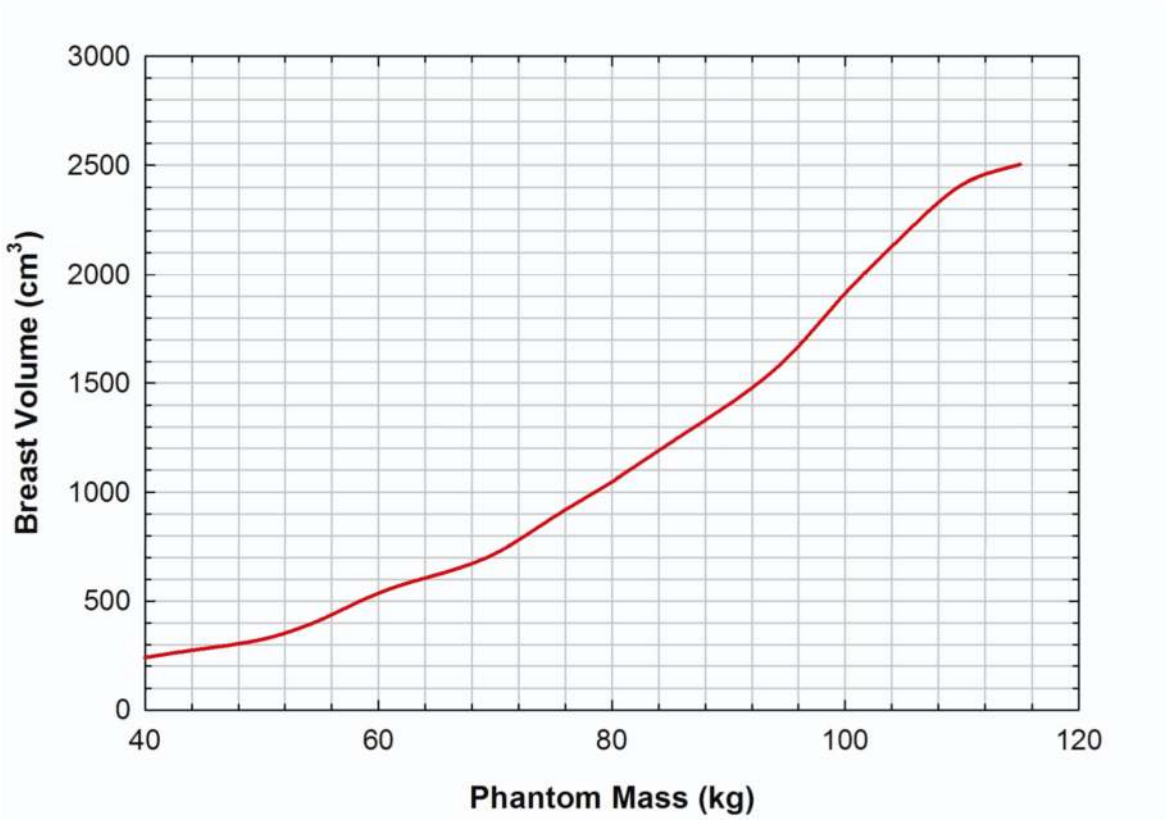

Figure 8.
Relative breast volumes as a function of weight for adult females at a standing height of 155 cm.

Table 1.

Mapping of reference phantoms and direction of height scaling performed to create the initial set of anchor phantoms by height for the various four patient- dependent libraries.

Phantom Height	Pediatric		Phantom Height	Adult	
(cm)	*Male*	*Females*	(cm)	*Males*	*Females*
185	UFHADM↑		190	UFHADM↑	
175	UFHADM↓	UFHADF↑	185	UFHADM↑	
165	UFH15M↓	UFHADF↑	180	UFHADM↑	
155	UFH15M↓	UFH15F↓	175	UFHADM↓	UFHADF↑
145	UFH10M↑	UFH10F↑	170	UFH15M↑	UFHADF↑
135	UFH10M↓	UFH10F↓	165	UFH15M↓	UFHADF↑
125	UFH10M↓	UFH10F↓	160	UFH15M↓	UFH15F↓
115	UFH05M↑	UFH05F↑	155		UFH15F↓
105	UFH05M↓	UFH05F↓	150		UFH15F↓
95	UFH05M↓	UFH05F↓			
85	UFH01M↑	UFH01F↑			

The naming convention for the UFphantom series begins with the identifier UFH (University of Florida Hybrid), followed by the reference phantom age in years (00, 01,05, 10, 15 and AD for adult) and then the phantom gender (M for male and F for female).

Table 2.

Comparison of the percentage of obese pediatric males and females as seen in the NHANES III (1988 – 1994) and NHANES IV (1999–2006) databases.

	Pediatric Males			Pediatric Females		
Height (cm)	**NHANES III**	**NHANES IV**	**% Difference**	**NHANES III**	**NHANES IV**	**% Difference**
85	3.8	2.2	–42%	3.4	3.1	–7%
95	4.5	5.5	22%	5.6	8.8	59%
105	6.7	12.3	84%	9.4	10.5	12%
115	13.3	14.5	9%	13.7	13.9	2%
125	12.5	17.9	44%	15.0	14.6	–2%
135	17.2	21.8	27%	17.1	18.9	10%
145	17.9	23.6	32%	15.8	21.2	34%
155	20.5	23.5	15%	16.9	19.9	18%
165	15.5	22.1	42%	16.9	21.6	28%
175	12.0	22.4	87%	14.7	26.0	76%
185	15.1	22.7	50%			
		Average	**34%**		***Average***	**23%**

Table 3.

Comparison of the percentage of obese adult males and females as seen in the NHANES III (1988 – 1994) and NHANES IV (1999–2006) databases.

	Adult Males			Adult Females		
Height (cm)	**NHANES III**	**NHANES IV**	**% Difference**	**NHANES III**	**NHANES IV**	**% Difference**
150				31.4	38.5	23%
155				30.7	40.3	31%
160	15.7	20.9	33%	30.2	38.8	29%
165	18.8	27.4	46%	28.6	37.1	30%
170	20.3	27.3	35%	27.5	34.6	26%
175	21.4	32.0	49%	29.3	31.9	9%
180	21.9	30.1	37%			
185	19.9	29.8	50%			
190	22.6	30.7	36%			
		Average	**41%**		***Average***	**24%**

Table 4.

Updated circumference values for the UF reference phantoms.

Phantom	Waist Circumference (cm)				Buttocks Circumference (cm)				Arm Circumference (cm)				Thigh Circumference (cm)			
	Current Reference	Updated Target	Revised Reference	% Diff	Current Reference	Updated Target	Revised Reference	% Diff	Current Reference	Updated Target	Revised Reference	% Diff	Current Reference	Updated Target	Revised Reference	% Diff
UFH05MF	57.7	52.5	54.2	3%	58.0	56.2	57.7	3%	14.8	17.5	17.5	0%	26.4	31.2	30.9	−1%
UFH10MF	70.9	61.2	63.1	3%	72.5	70.4	70.0	−1%	21.4	20.7	21.4	3%	31.6	38.2	37.6	−2%
UFH15M	89.9	72.2	74.4	3%	85.0	86.1	86.5	0%	27.2	26.6	27.2	2%	35.6	47.0	45.8	−3%
UFFH5F	76.9	73.4	75.9	3%	80.5	89.6	88.8	−1%	27.7	25.4	25.4	0%	43.5	46.7	46.4	−1%
UFHADM	97.9	89.3	92.0	3%	96.3	94.9	96.3	1%	27.3	30.8	31.1	1%	39.9	49.4	48.2	−2%
UFHADF	84.8	81.8	83.7	2%	93.8	95.9	93.8	−2%	29.0	27.8	28.0	1%	39.6	47.9	47.6	−1%

Table 5.

Select organ masses and their percent difference between pre- and post-voxelized values.

	Heart Wall			Lungs			Liver			Spleen			Thyroid			Kidney			Spongiosa		
Phantom	NURBS(g)	Voxelized (g)	% Difference	NURBS(g)	Voxelized (g)	% Difference	NURBS(g)	Voxelized (g)	% Difference	NURBS(g)	Voxelized (g)	% Difference	NURBS(g)	Voxelized (g)	% Difference	NURBS(g)	Voxelized (g)	% Difference	NURBS(g)	Voxelized (g)	% Difference
UFHPM - 135,25	99.8	99.1	0.6	299.6	293.2	2.2	591.4	589.3	0.4	57.0	56.7	0.5	5.6	5.5	2.0	129.8	129.2	0.5	1192.7	1203.0	−0.9
UFHPM - 135,30	99.8	99.1	0.6	299.6	293.2	2.2	591.4	589.3	0.4	57.0	56.7	0.5	5.6	5.5	2.0	129.8	129.2	0.5	1192.7	1203.0	−0.9
UFHPM - 135,35	111.7	110.8	0.8	335.5	328.4	2.2	662.2	660.5	0.3	63.8	63.7	0.2	6.3	6.3	0.4	145.4	144.5	0.6	1301.4	1314.7	−1.0
UFHPM - 135,40	111.7	110.8	0.8	335.5	328.4	2.2	662.2	660.5	0.3	63.8	63.7	0.2	6.3	6.3	0.4	145.4	144.5	0.6	1301.4	1314.7	−1.0
UFHPM - 135,45	111.7	110.8	0.8	335.5	328.4	2.2	662.2	660.5	0.3	63.8	63.7	0.2	6.3	6.3	0.4	145.4	144.5	0.6	1301.4	1314.7	−1.0
UFHPM - 135,50	111.7	110.8	0.8	335.5	328.4	2.2	662.2	660.5	0.3	63.8	63.7	0.2	6.3	6.3	0.4	145.4	144.5	0.6	1301.4	1314.7	−1.0
UFHAF -170,50	177.8	176.6	0.7	664.2	658.1	0.9	995.0	991.3	0.4	92.6	92.0	0.6	12.1	12.1	0.1	196.0	195.4	0.3	2129.1	2167.9	−1.8
UFHAF-170,55	202.1	201.2	0.5	755.1	747.9	1.0	1131.2	1126.9	0.4	105.2	104.3	0.9	13.7	13.8	−0.4	222.8	222.0	0.4	2381.1	2418.4	−1.5
UFHAF - 170,60	220.5	219.8	0.3	823.6	815.9	0.9	1233.9	1229.2	0.4	114.8	114.2	0.5	15.0	15.0	0.2	243.0	242.5	0.2	2571.3	2605.5	−1.3
UFHAF - 170,65	249.7	248.5	0.5	932.7	924.4	0.9	1397.3	1392.4	0.3	130.0	129.5	0.4	17.0	17.0	−0.4	275.2	274.6	0.2	2873.7	2909.8	−1.2
UFHAF - 170,70	273.2	271.7	0.6	1020.4	1011.1	0.9	1528.8	1523.0	0.4	142.2	141.2	0.7	18.6	18.6	−0.3	301.1	300.1	0.3	3117.1	3155.3	−1.2
UFHAF - 170,75	273.2	271.7	0.6	1020.4	1011.1	0.9	1528.8	1523.0	0.4	142.2	141.2	0.7	18.6	18.6	−0.3	301.1	300.1	0.3	3117.1	3155.3	−1.2
UFHAF - 170,80	273.2	271.7	0.6	1020.4	1011.1	0.9	1528.8	1523.0	0.4	142.2	141.2	0.7	18.6	18.6	−0.3	301.1	300.1	0.3	3117.1	3155.3	−1.2
UFHAF - 170,85	273.2	271.7	0.6	1020.4	1011.1	0.9	1528.8	1523.0	0.4	142.2	141.2	0.7	18.6	18.6	−0.3	301.1	300.1	0.3	3117.1	3155.3	−1.2
UFHAF -170,90	273.2	271.7	0.6	1020.4	1011.1	0.9	1528.8	1523.0	0.4	142.2	141.2	0.7	18.6	18.6	−0.3	301.1	300.1	0.3	3117.1	3155.3	−1.2
UFHAF -170,95	273.2	271.7	0.6	1020.4	1011.1	0.9	1528.8	1523.0	0.4	142.2	141.2	0.7	18.6	18.6	−0.3	301.1	300.1	0.3	3117.1	3155.3	−1.2
UFHAF -170,100	273.2	271.7	0.6	1020.4	1011.1	0.9	1528.8	1523.0	0.4	142.2	141.2	0.7	18.6	18.6	−0.3	301.1	300.1	0.3	3117.1	3155.3	−1.2
UFHAF -170,105	273.2	271.7	0.6	1020.4	1011.1	0.9	1528.8	1523.0	0.4	142.2	141.2	0.7	18.6	18.6	−0.3	301.1	300.1	0.3	3117.1	3155.3	−1.2
UFHAF -170,110	273.2	271.7	0.6	1020.4	1011.1	0.9	1528.8	1523.0	0.4	142.2	141.2	0.7	18.6	18.6	−0.3	301.1	300.1	0.3	3117.1	3155.3	−1.2
UFHAF - 170,115	273.2	271.7	0.6	1020.4	1011.1	0.9	1528.8	1523.0	0.4	142.2	141.2	0.7	18.6	18.6	−0.3	301.1	300.1	0.3	3117.1	3155.3	−1.2
UFHAF - 170,120	273.2	271.7	0.6	1020.4	1011.1	0.9	1528.8	1523.0	0.4	142.2	141.2	0.7	18.6	18.6	−0.3	301.1	300.1	0.3	3117.1	3155.3	−1.2
UFHAF - 170,125	273.2	271.7	0.6	1020.4	1011.1	0.9	1528.8	1523.0	0.4	142.2	141.2	0.7	18.6	18.6	−0.3	301.1	300.1	0.3	3117.1	3155.3	−1.2